HHS Public Access

Author manuscript

Circ Arrhythm Electrophysiol. Author manuscript; available in PMC 2016 December 01.

Published in final edited form as:

Circ Arrhythm Electrophysiol. 2015 December ; 8(6): 1325–1333. doi:10.1161/CIRCEP.115.002956.

Mechanisms for the Termination of Atrial Fibrillation by Localized Ablation: Computational and Clinical Studies

Wouter-Jan Rappel, PhD[1], **Junaid A. B. Zaman, MA, BMBCh**[2,3], and **Sanjiv M. Narayan, MD, PhD**[3]

[1]Department of Physics, University of California, San Diego, CA

[2]Department of Cardiology, Imperial College, University of London, London, United Kingdom

[3]Department of Medicine, Stanford University, Palo Alto, CA

Abstract

Background—Human atrial fibrillation (AF) can terminate after ablating localized regions, that supports the existence of localized rotors (spiral waves) or focal drivers. However, it is unclear why ablation near a spiral wave tip would terminate AF and not anchor reentry. We addressed this question by analyzing competing mechanisms for AF termination in numerical simulations, referenced to clinical observations.

Methods and Results—Spiral wave reentry was simulated in monodomain 2D myocyte sheets using clinically realistic rate-dependent values for repolarization and conduction. Heterogeneous models were created by introduction of parameterized variations in tissue excitability. Ablation lesions were applied as non-conducting circular regions. Computational models confirmed localized ablation may anchor spiral wave reentry, producing organized tachycardias. Several mechanisms also explained termination of AF to sinus rhythm. First, lesions may create an excitable gap vulnerable to invasion by fibrillatory waves. Second, ablation of rotors in regions of low-excitability (from remodeling) produced reentry in more excitable tissue allowing collision of wave-front and back. Conversely, ablation of rotors in high-excitability regions migrated spiral waves to less excitable tissue, where they detached to collide with non-conducting boundaries. Third, ablation may connect rotors to non-conducting anatomic orifices. Fourth, reentry through slow conducting channels may terminate if ablation closes these channels.

Conclusions—Limited ablation can terminate AF by several mechanisms. These data shed light on how clinical AF may be sustained in patients' atria, emphasizing heterogeneities in tissue excitability, slow-conducting channels and obstacles that are increasingly detectable in patients and should be the focus of future translational studies.

Correspondence: Wouter Jan Rappel, PhD, University of California San Diego, Urey Hall, Room 7242, San Diego, CA 92161, Tel: 858-822-1357, Fax: 858-534-7697, rappel@physics.ucsd.edu. Sanjiv M. Narayan, MD, Stanford University, 780 Welch Road MC-5773, Stanford, CA 94305, Tel: 650-498-8149, Fax: 650-724-6131, sanjiv1@stanford.edu.

Conflict of Interest Disclosures: *Dr. Rappel* reports being co-inventor on intellectual property owned by the University of California and licensed to Topera Medical, Inc. *Dr. Narayan* reports being co-inventor on intellectual property owned by the University of California and licensed to Topera Medical, Inc. Dr. Narayan reports having received consulting fees from Medtronic, Up to date, the American College of Cardiology and Janssen.

Keywords

rotor; ablation; treatment; computer-based model; reentry

Introduction

Atrial fibrillation (AF) is the commonest sustained arrhythmia, affecting 30 million patients worldwide [1]. AF increases morbidity and mortality yet therapy remains suboptimal, partly due to incomplete mechanistic understanding. Recent clinical studies show sources in the form of spiral wave reentry (rotors) or focal drivers sustaining AF[2, 3] and improved success with their ablation. However, in traditional basic science and simulation studies, ablation should not terminate such sources, instead even anchoring an AF rotor.

We studied mechanisms by which limited ablation may terminate AF, testing competing hypotheses in numerical models referenced to clinical observations. Our central hypothesis was that increasingly recognized functional and anatomic heterogeneities in human atria [3–8] may enable the elimination of AF sustaining regions by localized interventions.

In traditional theories, AF results from self-sustaining, non-hierarchical disordered waves, yet several clinical studies show AF may terminate with localized [2, 9] ablation. Strategies insufficient to limit critical mass such as focal lesions, lines, incomplete PV isolation or patchy ablation of complex electrograms [10–12] are often successful. New data from in vivo contact mapping [2] and the ECG-based inverse solution [3] and very recently optical mapping of human AF [13] support an alternative explanation – in which disordered activity is driven by localized rotors or focal sources. In the case of Focal Impulse and Rotor Mapping (FIRM), 2.1±1.1 cm^2 of tissue area is ablated per source [14] which, given 2–4 sources per patient, represents a small fraction of the ~100–130 cm^2 left atrial area in persistent AF patients [15]. These data challenge the non-hierarchical model of AF in which successful therapy must limit critical mass [16, 17].

Conversely, it is undefined how localized ablation eliminates reentrant sources for AF[18] without anchoring them. Termination of micro-reentrant AT with localized ablation without connecting to non-conducting obstacles or limiting critical mass [19] - a common result - offers a similar conundrum.

In this study, we numerically investigated the effects of ablation lesions on spiral wave reentry, incorporating increasingly appreciated non-uniformities in atrial physiology that may enable ablation to terminate AF, using clinical results to corroborate numerical findings.

Methods

Simulations

Simulations were carried out in isotropic 2-dimensional (2D) sheets using the monodomain equation:

$$\frac{dV}{dt} = \nabla \cdot D\nabla V - \frac{I_{ion}}{C_m} \quad (1)$$

Here, V is the membrane voltage, $C_m = 1\mu F/cm^2$ represents the membrane capacitance, D the diffusion tensor with diagonal entries of D=0.001 cm^2/ms, and I_{ion} the membrane currents. Membrane currents were implemented by the Fenton-Karma (FK) model [20, 21]. Parameter values for the FK model were chosen from set #3 of Ref [21] and excitability was modified through the parameter τ_d. As demonstrated [21], this set and variations in τ_d, can capture different spiral wave dynamics, including non-meandering and meandering spiral tips as well as spiral wave breakup. Notably, other parameter sets or detailed electrophysiological models give similar dynamics, and termination mechanisms discussed are not unique to a specific parameter set or model.

Eq. 1 was simulated on a square grid using a standard finite difference scheme with spatial discretization of 0.025 cm and time-step of 0.05 ms. These values of spatial and temporal discretization ensured conduction velocity (CV) and action potential durations were <3% of their converged values with resulting activation waves qualitatively unchanged [20]. During 1000ms cycle length pacing, CV and action potential duration for the parameter set were 42.5 cm/s and 270 ms, respectively. These values can be adjusted arbitrarily by multiplying all time constants and the diffusion coefficient with a constant. Computational details are detailed in Table 1.

Ablation lesions were modeled as circular regions of radius R_{abl} with zero conductivity, rendering the tissue inexcitable. R_{abl} was varied in in steps of 0.05 cm (range 0.2cm –1.0 cm). To account for zero-flux boundary conditions at the edge of the disk-like region we employ the phase-field method [22], which is well suited to model appropriate boundary conditions on curved interfaces while using a finite difference grid [23, 24]. The edges of the computational domain are assumed to have zero-flux boundary conditions unless otherwise specified.

Cardiac tissue can exhibit significant non-uniformities as a result of local differences in APD restitution, conduction [5–8], or fibrosis [4]. In our model, heterogeneity of tissue excitability was introduced by spatially varying one parameter of the FK model, τ_d. Low values correspond to highly excitable tissue while large values indicate reduced excitability. To vary this parameter in tissue, we defined two circles with radii R_1 and R_2, centered in the computational domain. The value of the excitability parameter was varied in a linear and radial fashion from τ_{d1} to τ_{d2}:

$$\tau_d = \tau_{d1} + (\tau_{d2} - \tau_{d1})(r - R_1)/(R_2 - R_1)$$

where *r* is location in the computational domain relative to its center.

Reentry arose from either cross-stimulation or using a broken wave as initial conditions. Several perturbations were then introduced as described in Results. Typical simulation times

ranged from 1–7mins on a workstation equipped with a dual 2.4 GHz quad-core Intel Xeon processor. Spiral tip trajectories were computed using a standard tracking algorithm [20].

Clinical Studies

An institutional review committee approved all clinical studies and subjects gave informed consent. The approach to mapping human AF and ablating localized sources has been detailed by our group [2] and others [3, 25–27]. We studied patients referred for ablation of symptomatic paroxysmal or persistent AF for standard indications[2]. After discontinuation of anti-arrhythmic medications[2], AF was recorded from bi-atrial multipolar contact catheters. Recordings were analyzed using methods described [2] to interpret electrograms based on human repolarization[28] and conduction[5, 7] dynamics.

Electrical rotors were defined as phase singularities that radiate electrical waves into surrounding tissue at high rate causing wavebreak into fibrillation [29], while focal impulses showed centrifugal activation from an origin. AF sources identified using contact mapping precess ('wobble') in reproducible and limited areas [14] for long periods of time[30], while drivers mapped by the inverse solution also occur in reproducible and limited regions for days[3].

Ablation of each AF source involved application of radiofrequency energy to the ≈2–3 cm^2 precession area [14]. This process (Focal Impulse and Rotor Modulation, FIRM) was repeated for each source (2.1±1.1 per patient)[2]. Subsequent clinical care included conventional ablation[10]. In this report we focus only on the impact of limited FIRM-guided ablation to acutely terminate AF. We illustrate modeling-predicted mechanisms of AF termination with examples from our experience of FIRM-guided ablation.

Results

Computational simulations revealed several mechanisms by which limited ablation interfered with spiral wave reentry, converting AF to organized tachycardias, or terminating AF to sinus rhythm. These mechanisms were consistent with several observed clinical cases of rotor targeted (FIRM-guided) ablation.

Conversion of AF to AT

Targeted ablation (a non-conducting obstacle) may pin a spiral wave to fixed reentry around the obstacle. Figure 1A shows a numerical example of a spiral wave with meander (green line, shown for ~ 900 ms) causing AF in surrounding tissue. An ablation lesion (blue disk) alters tip trajectory (red line) and after ~ 1200 ms the spiral tip is stably anchored at the lesion. This spiral wave produces regular atrial tachycardia (AT) with cycle length 210 ms. As reported in other computational studies [31, 32], spiral wave anchoring requires a minimum lesion size, dependent on location. Figure 1B presents more complex activation with three co-existing meandering spiral waves, created by increasing the computational domain and introducing periodic boundary conditions in the horizontal direction (see Table 1 for details). The rotors were initiated using conditions containing broken waves and coexisted for an extended duration (>4 s). An ablation lesion anchors one of the spirals and, after a period of

~ 2000 ms, annihilation of other spirals (Figure 1C). Activation is now regular and consistent with AT of cycle length 230 ms.

Next, simulations revealed several mechanisms enabling limited ablation to terminate spiral wave reentry, consistent with conversion of AF to sinus rhythm.

Elimination of reentry by creation of an excitable gap

First, we studied the impact of ablation creating an excitable gap near the rotor core. Figure 2A shows a snapshot of simulations in which the excitability parameter τ_d produced multiple spiral waves, τ_d=0.34. Creating a lesion (Figure 2B) anchored one spiral wave leaving a small excitable gap (Figure 2C). Activation from surrounding fibrillatory waves invaded this excitable gap, with a stochastic likelihood of wave collision causing block and terminating reentry (Figure 2D and Supplementary Movie 1). We have verified other values of τ_d and domain sizes display the same termination mechanism. For example, simulations using τ_d=0.32 in a 5x5cm domain and τ_d=0.36 in a 7.5x7.5cm result in spiral wave dislodgement by surrounding waves, followed by termination.

Elimination of reentry related to gradients in tissue excitability

To address mechanisms based on spatial heterogeneities in tissue, we varied the FK model excitability parameter, τ_d, in a radial fashion (see methods). Initially, we created a spiral wave stably attached to a non-conducting zone with a radius of 0.4 cm (Figure 3) and investigated two scenarios: one in which excitability increased with distance from the non-conducting zone and one in which it decreased. An ablation lesion introduced over the initial non-conducting zone but of larger radius was able to unpin the anchored spiral in both scenarios.

Figure 3A–B illustrates the first scenario, with excitability higher within the dashed circle than in surrounding tissue (τ_{d1}=0.3 to τ_{d2}=0.42, with corresponding CVs of 36.7 cm/s and 26.3 cm/s, respectively). Ablating the heterogeneous high-excitability domain results in a non-conducting zone (radius 0.8 cm), detachment of the spiral wave, consequent migration and collision with anatomic obstacles (modeled as no-flux boundaries). This resulted in termination of the rotor and AF (Supplementary Movie 2). Varying ablation radius in steps of 0.05 cm revealed minimum ablation radius for the parameters in Fig. 3A as 0.65 cm. We have verified other combinations of τ_{d1}, τ_{d2}, R_1, and R_2, result in successful termination as well. For example, creating sufficiently large ablation lesions when changing either τ_{d1} (to 0.25) or R_1 (to 0.6 cm) only causes spiral wave termination. Clearly, minimum ablation size will depend on precise parameter values but the qualitative termination behavior of Fig. 3 is insensitive to parameter choices.

Figure 3C–E illustrates the second scenario when ablation may terminate a spiral wave whose tip is located in a region of low excitability (R_1=0.4 cm, τ_{d1} = 0.35 and CV=33.0 cm/s) surrounded by higher excitability (τ_{d2} = 0.25 and CV=42.6 cm/s). Initially, the activation front is anchored at a small, circular non-conducting obstacle. Creating an ablation lesion of larger radius results in the activation front propagating in tissue with higher excitability and correspondingly higher wave speed, allowing activation front and

back to eventually meet, leading to block (double bars in Figure 3E). This results in detachment of the wave front and termination of reentry (Supplementary Movie 3). As in the first scenario, this mechanism is insensitive to precise parameter values. Using different values of τ_{d1}, τ_{d2}, R_1, and R_2 (for example, τ_{d1}=0.40, τ_{d2}=0.20, R_1=0.4 cm, and R_2=2.0 cm or τ_{d1}=0.40, τ_{d2}=0.20, R_1=0.3 cm, and R_2=1.5 cm) can result in the termination mechanisms of Fig. 3C–E.

Terminating reentry by creating a barrier to non-conducting obstacles

Targeted ablation could also terminate spiral waves if lesions connect to a large non-conducting obstacle (e.g. an anatomic orifice or a large scar). Figure 4A shows a spiral wave with tip trajectory close to a non-conducting zone (the lower boundary of the simulation domain). Targeted ablation connecting the spiral wave core to this obstacle terminates reentry. This is shown in the snapshots displayed in panels B–C where we highlight wave block occurring in the gaps between lesions. The lesions prevent the wave from rotating (B) and push it towards the non-conducting boundary where it extinguishes (C). Note that ablation lesions need not overlap, as isthmuses require a minimum size to support wave propagation [33], approximately 0.05 cm in our simulation.

Terminating reentry by ablation of an isthmus for reentry

In computational models, AF often exhibits paired spiral waves of opposite chirality, with one spiral extinguishing. We modeled a scenario whereby reentry is supported by a slow-conducting isthmus between non-conducting zones (hatched regions in Figure 5). The isthmus region has a linear gradient in diffusion constant ranging from D=0.0002 cm^2/ms (left-side) to D=0.00005 cm^2/ms (right-side). This approximately 10-fold lower diffusion constant results in a CV approximately 4 times smaller than surrounding tissue (9.4 cm/s vs. 36.6 cm/s for D=0.0001 cm^2/ms, τ_d=0.30). The mismatch in CV between isthmus and surrounding tissue creates figure-of-eight reentry (green arrows in Figure 5D and Supplementary Movie 4). In this scenario, ablating the slow conduction zone blocks the reentry pathway, terminating reentry.

Clinical cases illustrating various mechanisms of AF termination

Observations in several patients support the modeling-predicted mechanisms of AF termination. Figure 6 shows atrial propagation in a 67 year old man with left atrial diameter 62 mm, persistent AF and no prior ablation, in whom brief ablation (cumulative duration 6 minutes for diameter ≈2 cm) at a counter clockwise left atrial rotor anchored spiral wave reentry to produce organized tachycardia at this region. The AT was then ablated to sinus rhythm. This example is consistent with the mechanism in Figure 1.

Figure 7 illustrates a 85 year old man with a long history of AF but no prior ablation, in whom ablation at the first catheter position for less than 1 minute (<1 cm diameter) at the rotor core destabilized the previously stable rotor, terminating AF to sinus rhythm. This is consistent with the mechanism in figure 3 whereby the destabilized spiral wave tip may collide with the mitral annulus, left inferior pulmonary vein or other structural boundary.

Figure 8 shows cases of AF rotors near non-conducting boundaries. In figure 8A, rotor ablation near the left superior pulmonary vein, during the first ablation of a patient with persistent AF, enabled AF termination after a cumulative of 2.5 minutes energy delivery (≈1.3 cm diameter). In figure 8B, in a gentleman with AF despite prior left atrial ablation (none in right atrium), ablation commenced at a rotor near the inferior vena cava. The first lesions delivered terminated AF to sinus rhythm after a total cumulative ablation time of 48 seconds (<1 cm diameter). These data are consistent with ablation connecting rotor cores to these non-conducting boundaries as illustrated in Figure 4.

Finally, the Supplementary Figure illustrates a case of paired rotors of opposite chirality in the right atrium in a 63 year old man with persistent AF, left atrial diameter 54 mm and a dual chamber pacemaker. We performed ablation at the medial rotor core only, as the lateral core lay at a pacemaker lead site.

Discussion

This work provides a novel theoretical foundation for AF, illustrating for the first time how limited ablation targeted to the site(s) of localized sources can terminate AF to sinus rhythm or organized atrial tachycardia. Although the clinical literature is replete with cases where limited ablation terminates AF, there has previously been no theoretical foundation explaining this phenomenon – using either non-hierarchical (i.e. multiwavelet reentry) or hierarchical (i.e. source) models of AF. The present study illustrates how increasingly recognized structural heterogeneities and functional non-uniformities in remodeled human atria may enable ablation to terminate AF, by non-uniform excitability, conduction, repolarization and non-conducting obstacles. Clinically, these data may help to guide improved ablation strategies and, mechanistically, suggest specific approaches to modify AF substrates by ionic, anti-fibrotic or regenerative therapies.

Disorganized or localized mechanisms sustaining AF: A fundamental dilemma

Whether AF is maintained by non-hierarchical self-sustaining disorganization or is hierarchical such that localized regions [29] drive disorganization remains a central mechanistic debate. Answers to this question will affect decision making in AF therapy.

Disorganized sustaining mechanisms were proposed by Moe et al. [29] and are supported by surgical studies demonstrating re-entry without hierarchy using recording plaques [34]. However, these studies have limitations as clinical AF signals may reflect non-local activation[35], complex signals are often ignored[34] and plaques only simultaneously map small regions (<10–20% of both atria). This mechanism also cannot reconcile how AF is modulated by limited ablation[9, 25], why outcomes are worse when performing more ablation[12] (i.e. undergoing greater mass reduction), and data directly challenging the critical mass concept[17].

Localized sources for fibrillation were demonstrated directly by the pioneering work of Jalife et al. in the early 1990s [29] and by recent optical mapping studies in human AF [13]. Sources readily explain modulation of AF by ablation[2, 9], insufficient to limit critical mass [10, 12], AF termination by localized intervention [36] and increasing data showing

stability of propagation. A hierarchical model also explains success during extensive ablation – if it coincidentally modifies sources [37]. One major question for the source hypothesis is how localized ablation at rotors can abolish AF[18]. The present study provides the first potential answers to that question.

Reconciling our studies with prior work

First, the present study confirms prior computational [31, 32, 38, 39] and *in vitro* [40–42] studies where limited ablation converted an AF rotor to anatomical reentry. This is consistent with clinical cases (Figure 6) using FIRM [2] or an ECG-based inverse solution[3], supporting the localized source hypothesis. Studies are required to exclude ablation modulating "high densities of multiple wavelets" [18], although this would not explain why the unablated lower density wavelets do not perpetuate AF.

Second, this study provides the first set of mechanisms to explain how limited ablation terminates AF directly to sinus rhythm. Most numerical simulations studied anchoring of spiral waves to obstacles in uniform tissue [31, 32, 38, 39, 43], revealing how both low and high excitability limit the minimum obstacle size around which reentry is stable. In tissue with uniformly low excitability, spiral tips cannot follow trajectories with high curvature[44]. Thus, stable attachment to a circular obstacle requires a minimum radius – if smaller, spiral waves will detach. In tissue with uniformly high excitability, the CV determines the minimum size of an anchoring obstacle. The CV is large (small) for high (low) excitability and, accordingly, highly excitable tissue can only support activation if the path around the obstacle has a minimum size – if smaller, activating 'head meets tail', detaching wavefronts. Thus, in uniform tissue, it is unlikely that limited ablation can dislodge an anchored spiral wave.

However, our study shows that incorporating well-recognized non-uniformities in atrial tissue reveals several mechanisms whereby limited targeted ablation can terminate AF rotors. Non-uniformities in atrial tissue are ubiquitous and possibly due to regional variations in APD restitution, conduction [5–8], fibrosis [4] or fiber architecture [13]. In the scenarios studied (Figure 3), the initial condition consists of an activation front rotating around a small obstacle. The tissue properties close to this obstacle were chosen to differ from those further away. Note this initial condition is stable due to this spatial heterogeneity: choosing uniform excitability equal to the excitability far from the obstacle would result in detachment in both cases. In the first scenario (Figure 3A–B), stable reentry around an obstacle in tissue with an excitability equal to that of the tissue further from the initial obstacle (τ_{d2} = 0.42) requires a minimum obstacle radius of R=1.9 cm, much larger than a single ablation lesion (typical size 0.5–0.7 cm). Tissue with excitability corresponding to the parameter value at the periphery of Figure 3C–E (τ_{d2} = 0.25) requires a minimum radius of R=1.2 cm, again larger than a lesion. This may explain how hyperkalemia terminates fibrillatory rotors [45].

Validating results from this modeling study with clinical observations

Ablation may lengthen wavepath around lesions, analogous to micro-reentrant AT[46]. A rapid micro-reentrant source driving AF with fibrillatory conduction may terminate if the

excitable gap is invaded by fibrillatory waves. The effects of pacing on spiral tips has been studied before [47] and we recently demonstrated in a case study of AF propagation using patient-specific geometries that fibrillatory waves can invade an excitable gap [48]. This model agrees with clinical observation, where even if AF is inducible it may be shorter, with recurrence relating to ATs depending on the extent of ablated tissue[3, 4, 14]. Studies are needed to further define our description of conduction properties at sites of rotors and surrounding tissue[7] to identify patients in which gradients of excitability may operate.

The proposed mechanism of joining the rotor site to a non-conducting obstacle or eliminating a non-conducting channel both require direct clinical validation. However, Figure 8 illustrates rotors whose location would easily enable targeted ablation to connect to non-conducting boundaries including ‘functional’ boundaries. Supplementary Figure 1 shows figure-of-8 activation through slow-conducting channels, that may occur in relation to fibrosis or other forms of atrial remodeling, awaiting clinical mapping validation.

Limitations

There are several limitations of this study. First, it was performed in computational grids not accounting for geometrical curvature, that may provide additional mechanisms for ablation to terminate AF [29]. Second, we used the FK model for computational efficiency, so our study was not designed to explore effects of derangements in specific ion channels or drugs on AF. Third, simulations were performed in isotropic domains, whereas fiber anisotropy can affect spiral tip dynamics[29, 48]. Fourth, ablation lesions were modeled as discrete obstacles to activation and conduction, while in practice the necrotic core of an ablation lesion is surrounded by a penumbra of inflammation that may shorten APD and alter wave dynamics. Future studies should attempt to quantify such inflammation so that it may be incorporated. Fifth, simulations were carried out in 2D sheets that did not include transmural components. Indeed, epicardial and endocardial differences in cellular and fiber properties were recently shown in optical mapping of human AF [13]. The study found stable rotors (≈1 cm^2 precession areas on the endocardium), terminated by localized ablation, but less stability on the epicardium, where they appeared as focal breakthroughs. It remains to be seen if this transmural difference is consistent. We did not model the impact of ablation on potential focal sources for AF, since this is mechanistically straightforward. Clinically, we were unable to directly register clinical cases with computational models. Although FIRM-based mapping is sufficient to map human AF at the resolution required for ablation [49], it is insufficient to map the dynamics of the rotor core during ablation. In the present study, clinical data illustrate model predictions, and are not used to present a definitive mechanistic proof or a relationship to the long-term results of rotor ablation as shown by others[27, 50] and for which randomized trials are ongoing.

Conclusions

This study proposes novel mechanisms by which limited ablation can terminate human AF. These data illustrate for the first time how targeted ablation may interact dynamically with the anatomical locations of rotors and with tissue characteristics of non-uniform excitability, slow conduction and non-conducting boundaries. Future translational studies should focus

on mapping and quantifying these tissue heterogeneities in remodeled atria in individual patients in order to improve therapy.

Supplementary Material

Refer to Web version on PubMed Central for supplementary material.

Acknowledgments

Funding Sources: This work was supported by National Institutes of Health Grants R01 HL122384 (WJR), R01 HL83359 and K24 HL103800 (SMN), and by a British Heart Foundation fellowship (FS/14/46/30907) to JABZ.

References

1. Chugh SS, Havmoeller R, Narayanan K, Singh D, Rienstra M, Benjamin EJ, Gillum RF, Kim YH, McAnulty JH Jr, Zheng ZJ, Forouzanfar MH, Naghavi M, Mensah GA, Ezzati M, Murray CJ. Worldwide epidemiology of atrial fibrillation: a Global Burden of Disease 2010 Study. Circulation. 2014; 129:837–847. [PubMed: 24345399]
2. Narayan SM, Krummen DE, Shivkumar K, Clopton P, Rappel W-J, Miller J. Treatment of Atrial Fibrillation by the Ablation of Localized Sources: The Conventional Ablation for Atrial Fibrillation With or Without Focal Impulse and Rotor Modulation: CONFIRM Trial. J Am Coll Cardiol. 2012; 60:628–636. [PubMed: 22818076]
3. Haissaguerre M, Hocini M, Denis A, Shah AJ, Komatsu Y, Yamashita S, Daly M, Amraoui S, Zellerhoff S, Picat MQ, Quotb A, Jesel L, Lim H, Ploux S, Bordachar P, Attuel G, Meillet V, Ritter P, Derval N, Sacher F, Bernus O, Cochet H, Jais P, Dubois R. Driver domains in persistent atrial fibrillation. Circulation. 2014; 130:530–538. [PubMed: 25028391]
4. Marrouche NF, Wilber D, Hindricks G, Jais P, Akoum N, Marchlinski F, Kholmovski E, Burgon N, Hu N, Mont L, Deneke T, Duytschaever M, Neumann T, Mansour M, Mahnkopf C, Herweg B, Daoud E, Wissner E, Bansmann P, Brachmann J. Association of atrial tissue fibrosis identified by delayed enhancement MRI and atrial fibrillation catheter ablation: the DECAAF study. JAMA. 2014; 311:498–506. [PubMed: 24496537]
5. Lalani G, Schricker A, Gibson M, Rostamanian A, Krummen DE, Narayan SM. Atrial Conduction Slows Immediately Before the Onset of Human Atrial Fibrillation: A Bi-Atrial Contact Mapping Study of Transitions to Atrial Fibrillation. J Am Coll Cardiol. 2012; 59:595–606. [PubMed: 22300695]
6. Markides V, Schilling RJ, Yen Ho S, Chow AWC, Davies DW, Peters NS. Characterization of Left Atrial Activation in the Intact Human Heart. Circulation. 2003; 107:733–739. [PubMed: 12578877]
7. Schricker A, Rostamian A, Lalani G, Krummen DE, Narayan SM. Human Atrial Fibrillation Initiates by Organized Not Disorganized Mechanisms. Circ Arrhythm Electrophysiol. 2014; 7:816–824. [PubMed: 25217042]
8. Stiles MK, John B, Wong CX, Kuklik P, Brooks AG, Lau DH, Dimitri H, Roberts-Thomson KC, Wilson L, De Sciscio P, Young GD, Sanders P. Paroxysmal lone atrial fibrillation is associated with an abnormal atrial substrate: characterizing the “second factor”. J Am Coll Cardiol. 2009; 53:1182–1191. [PubMed: 19341858]
9. Herweg B, Kowalski M, Steinberg JS. Termination of persistent atrial fibrillation resistant to cardioversion by a single radiofrequency application. Pacing Clin Electrophysiol. 2003; 26:1420–1423. [PubMed: 12822761]
10. Calkins CH. 2012 HRS/EHRA/ECAS Expert Consensus Statement on Catheter and Surgical Ablation of Atrial Fibrillation: Recommendations for Patient Selection, Procedural Techniques, Patient Management and Follow-up, Definitions, Endpoints, and Research Trial Design. Heart Rhythm. 2012; 9:632–696. [PubMed: 22386883]
11. Nademanee K, McKenzie J, Kosar E, Schwab M, Sunsaneewitayakul B, Vasavakul T, Khunnawat C, Ngarmukos T. A new approach for catheter ablation of atrial fibrillation: mapping of the electrophysiologic substrate. J Am Coll Cardiol. 2004a; 43:2044–2053. [PubMed: 15172410]

12. Haissaguerre M, Sanders P, Hocini M, Takahashi Y, Rotter M, Sacher F, Rostock T, Hsu L-F, Bordachar P, Reuter S, Roudaut R, Clementy J, Jais P. Catheter Ablation of Long-Lasting Persistent Atrial Fibrillation: Critical Structures for Termination. J Cardiovasc Electrophysiol. 2005; 16:1125–1137. [PubMed: 16302892]
13. Hansen BJ, Zhao J, Csepe TA, Moore BT, Li N, Jayne LA, Kalyanasundaram A, Lim P, Bratasz A, Powell KA, Simonetti OP, Higgins RS, Kilic A, Mohler PJ, Janssen PM, Weiss R, Hummel JD, Fedorov VV. Atrial fibrillation driven by micro-anatomic intramural re-entry revealed by simultaneous sub-epicardial and sub-endocardial optical mapping in explanted human hearts. Eur Heart J. 2015 Jun 8. pii: ehv233 Epub ahead of print.
14. Narayan SM, Shivkumar K, Krummen DE, Miller JM, Rappel W-J. Panoramic Electrophysiological Mapping But Not Individual Electrogram Morphology Identifies Sustaining Sites for Human Atrial Fibrillation (AF Rotors and Focal Sources Relate Poorly to Fractionated Electrograms). Circ Arrhythm Electrophysiol. 2013; 6:58–67. [PubMed: 23392583]
15. Jadidi AS, Cochet H, Shah AJ, Kim SJ, Duncan E, Miyazaki S, Sermesant M, Lehrmann H, Lederlin M, Linton N, Forclaz A, Nault I, Rivard L, Wright M, Liu X, Scherr D, Wilton SB, Roten L, Pascale P, Derval N, Sacher F, Knecht S, Keyl C, Hocini M, Montaudon M, Laurent F, Haissaguerre M, Jais P. Inverse relationship between fractionated electrograms and atrial fibrosis in persistent atrial fibrillation: combined magnetic resonance imaging and high-density mapping. J Am Coll Cardiol. 2013; 62:802–812. [PubMed: 23727084]
16. Zou R, Kneller J, Leon LJ, Nattel S. Substrate size as a determinant of fibrillatory activity maintenance in a mathematical model of canine atrium. Am J Physiol Heart Circ Physiol. 2005; 289:H1002–1012. [PubMed: 15849234]
17. Vaidya D, Morley GE, Samie FH, Jalife J. Reentry and fibrillation in the mouse heart. A challenge to the critical mass hypothesis. Circ Res. 1999; 85:174–181. [PubMed: 10417399]
18. Carrick RT, Benson B, Habel N, Bates OR, Bates JH, Spector PS. Ablation of multiwavelet re-entry guided by circuit-density and distribution: maximizing the probability of circuit annihilation. Circ Arrhythmia Electrophysiol. 2013; 6:1229–1235.
19. Markowitz SM, Nemirovksy D, Stein KM, Mittal S, Iwai S, Shah BK, Dobesh DP, Lerman BB. Adenosine-insensitive focal atrial tachycardia: evidence for de novo micro-re-entry in the human atrium. J Am Coll Cardiol. 2007; 49:1324–1333. [PubMed: 17394965]
20. Fenton F, Karma A. Vortex dynamics in three-dimensional continuous myocardium with fiber rotation: Filament instability and fibrillation. Chaos. 1998; 8:20–47. [PubMed: 12779708]
21. Fenton FH, Cherry EM, Hastings HM, Evans SJ. Multiple mechanisms of spiral wave breakup in a model of cardiac electrical activity. Chaos. 2002; 12:852–892. [PubMed: 12779613]
22. Karma A, Rappel WJ. Phase-field method for computationally efficient modeling of solidification with arbitrary interface kinetics. Phys Rev E Stat Phys Plasmas Fluids Relat Interdiscip Topics. 1996; 53:R3017–R3020. [PubMed: 9964755]
23. Kockelkoren J, Levine H, Rappel W-J. Computational approach for modeling intra-and extracellular dynamics. Phys Rev E Stat Nonlin Soft Matter Phys. 2003; 68:037702. [PubMed: 14524934]
24. Fenton FH, Cherry EM, Karma A, Rappel W-J. Modeling wave propagation in realistic heart geometries using the phase-field method. Chaos. 2005; 15:013502.
25. Shivkumar K, Ellenbogen KA, Hummel JD, Miller JM, Steinberg JS. Acute Termination of Human Atrial Fibrillation by Identification and Catheter Ablation of Localized Rotors and Sources: First Multicenter Experience of Focal Impulse and Rotor Modulation (FIRM) Ablation. J Cardiovasc Electrophysiol. 2012; 23:1277–1285. [PubMed: 23130890]
26. Lin YJ, Lo MT, Lin C, Chang SL, Lo LW, Hu YF, Hsieh WH, Chang HY, Lin WY, Chung FP, Liao JN, Chen YY, Hanafy D, Huang NE, Chen SA. Prevalence, characteristics, mapping, and catheter ablation of potential rotors in nonparoxysmal atrial fibrillation. Circ Arrhythm Electrophysiol. 2013; 6:851–858. [PubMed: 23983246]
27. Miller JM, Kowal RC, Swarup V, Daubert JP, Daoud EG, Day JD, Ellenbogen KA, Hummel JD, Baykaner T, Krummen DE, Narayan SM, Reddy VY, Shivkumar K, Steinberg JS, Wheelan KR. Initial Independent Outcomes from Focal Impulse and Rotor Modulation Ablation for Atrial Fibrillation: Multicenter FIRM Registry. J Cardiovasc Electrophys. 2014; 25:921–929.

28. Narayan SM, Franz MR, Clopton P, Pruvot EJ, Krummen DE. Repolarization Alternans Reveals Vulnerability to Human Atrial Fibrillation. Circulation. 2011; 123:2922–2930. [PubMed: 21646498]
29. Pandit SV, Jalife J. Rotors and the dynamics of cardiac fibrillation. Circ Res. 2013; 112:849–862. [PubMed: 23449547]
30. Swarup V, Baykaner T, Rostamian A, Daubert JP, Hummel J, Krummen DE, Trikha R, Miller JM, Tomassoni GF, Narayan SM. Stability of rotors and focal sources for human atrial fibrillation: focal impulse and rotor mapping (FIRM) of AF sources and fibrillatory conduction. J Cardiovasc Electrophysiol. 2014; 25:1284–1292. [PubMed: 25263408]
31. Zou X, Levine H, Kessler DA. Interaction between a drifting spiral and defects. Phys Rev E Stat Phys Plasmas Fluids Relat Interdiscip Topics. 1993; 47:R800–R803. [PubMed: 9960165]
32. Olmos D. Reflection and attachment of spirals at obstacles for the Fitzhugh-Nagumo and Beeler-Reuter models. Phys Rev E Stat Nonlin Soft Matter Phys. 2010; 81:041924. [PubMed: 20481770]
33. Cabo C, Pertsov AM, Baxter WT, Davidenko JM, Gray RA, Jalife J. Wave-front curvature as a cause of slow conduction and block in isolated cardiac muscle. Circ Res. 1994; 75:1014–1028. [PubMed: 7525101]
34. Allessie MA, de Groot NM, Houben RP, Schotten U, Boersma E, Smeets JL, Crijns HJ. Electropathological substrate of long-standing persistent atrial fibrillation in patients with structural heart disease: longitudinal dissociation. Circ Arrhythm Electrophysiol. 2010; 3:606–615. [PubMed: 20719881]
35. Narayan SM, Wright M, Derval N, Jadidi A, Forclaz A, Nault I, Miyazaki S, Sacher F, Bordachar P, Clementy J, Jais P, Haissaguerre M, Hocini M. Classifying Fractionated Electrograms in Human Atrial Fibrillation Using Monophasic Action Potentials and Activation Mapping: Evidence for Localized Drivers, Rate Acceleration and Non-Local Signal Etiologies. Heart Rhythm. 2011a; 8:244–253. [PubMed: 20955820]
36. Tzou WS, Saghy L, Lin D. Termination of persistent atrial fibrillation during left atrial mapping. J Cardiovasc Electrophysiol. 2011; 22:1171–1173. [PubMed: 21539640]
37. Narayan SM, Clopton P, Krummen DE, Shivkumar K, Miller J. Direct or Concidental Ablation of Localized Sources May Explain the Success of Atrial Fibrillation Ablation. On Treatment Analysis from the CONFIRM Trial. J Am Coll Cardiol. 2013a; 62:138–147. [PubMed: 23563126]
38. Xie F, Qu Z, Garfinkel A. Dynamics of reentry around a circular obstacle in cardiac tissue. Phys Rev E Stat Nonlin Soft Matter Phys. 1998; 58:6355–6358.
39. McDowell KS, Vadakkumpadan F, Blake R, Blauer J, Plank G, Macleod RS, Trayanova NA. Mechanistic inquiry into the role of tissue remodeling in fibrotic lesions in human atrial fibrillation. Biophys J. 2013; 104:2764–2773. [PubMed: 23790385]
40. Lim Z, Maskara B, Aguel F, Emokpae RJ, Tung L. Spiral wave attachment to millimeter-sized obstacles. Circulation. 2006; 114:2113–2121. [PubMed: 17088465]
41. Cysyk J, Tung L. Electric field perturbations of spiral waves attached to millimeter-size obstacles. Biophys J. 2008; 94:1533–41. [PubMed: 17921205]
42. Ikeda T, Yashima M, Uchida T, Hough D, Fishbein MC, Mandel WJ, Chen PS, Karagueuzian HS. Attachment of meandering reentrant wave fronts to anatomic obstacles in the atrium. Role of the obstacle size. Circ Res. 1997; 81:753–764. [PubMed: 9351449]
43. Dang L, Virag N, Ihara Z, Jacquemet V, Vesin J, Schlaepfer J, Ruchat P, Kappenberger L. Evaluation of ablation patterns using a biophysical model of atrial fibrillation. Ann Biomed Eng. 2005; 33:465–474. [PubMed: 15909652]
44. Cabo C, Pertsov AM, Davidenko JM, Baxter WT, Gray RA, Jalife J. Vortex shedding as a precursor of turbulent electrical activity in cardiac muscle. Biophys J. 1996; 70:1105–1111. [PubMed: 8785270]
45. Pandit SV, Warren M, Mironov S, Tolkacheva EG, Kalifa J, Berenfeld O, Jalife J. Mechanisms underlying the antifibrillatory action of hyperkalemia in Guinea pig hearts. Biophys J. 2010; 98:2091–2101. [PubMed: 20483316]
46. El Haddad M, Houben R, Tavernier R, Duytschaever M. Stable reentrant circuit with spiral wave activation driving atrial tachycardia. Heart Rhythm. 2014; 11:716–718. [PubMed: 24389576]

47. Davidenko JM, Salomonsz R, Pertsov AM, Baxter WT, Jalife J. Effects of pacing on stationary reentrant activity. Theoretical and experimental study. Circ Res. 1995; 77:1166–1179. [PubMed: 7586230]

48. Gonzales MJ, Vincent KP, Rappel W-J, Narayan SM, McCulloch AD. Structural Contributions to Fibrillatory Rotors in a Patient-Derived Computational Model of the Atria. Europace. 2014; 16:iv3–iv10. [PubMed: 25362167]

49. Rappel W-J, Narayan SM. Theoretical Considerations for Mapping Activation in Human Cardiac Fibrillation. Chaos. 2013; 23:023113. [PubMed: 23822478]

50. Narayan SM, Baykaner T, Clopton P, Schricker A, Lalani G, Krummen DE, Shivkumar K, Miller JM. Ablation of Rotor and Focal Sources Reduces Late Recurrence of Atrial Fibrillation Compared to Trigger Ablation Alone: Extended Followup of the CONFIRM (CONventional ablation with or without Focal Impulse and Rotor Modulation) Trial. J Am Coll Cardiol. 2014; 63:1761–1768. [PubMed: 24632280]

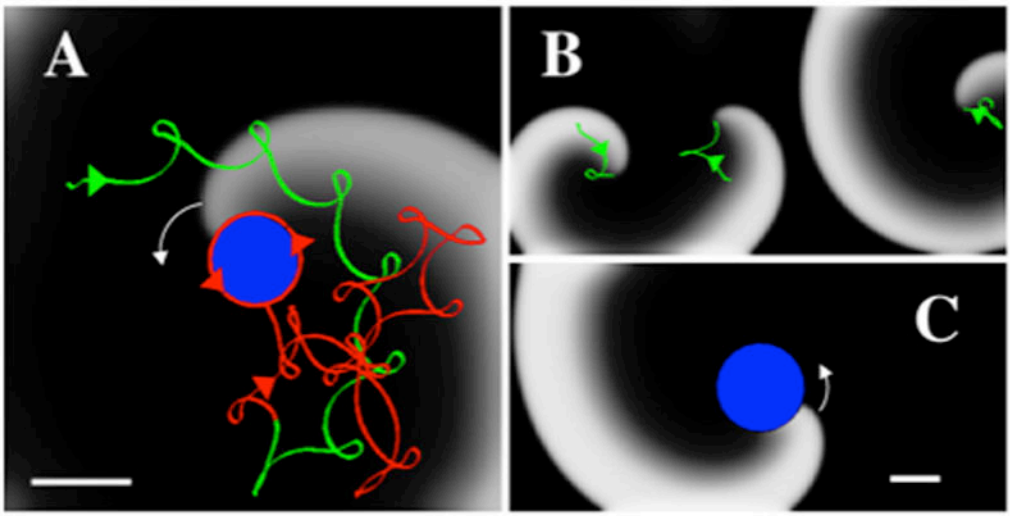

Figure 1.

Conversion of AF to AT. A. Snapshot of anchoring of a counter clockwise spiral wave (white arrow) by introduction of a non-conducting ablation lesion. Activation is shown using a gray scale with white indicating activated tissue and black indicating recovered tissue. The spiral tip trajectory before the introduction of the lesion is shown in green and meanders, resulting in AF-like activation. The creation of a lesion (blue disk) progressively anchors the trajectory (shown as the red trajectory) that converges to a regular AT (counterclockwise red arrows). The tissue has as size 5cmx5cm, and R_{abl}=0.4 cm. The direction of the tip trajectories are indicated by arrows. B, C. Snapshots before (B) and after (C) the introduction of a circular lesion (blue, R_{abl}=1 cm) in a larger computational domain (10cmx5cm) with period boundary conditions in the horizontal direction. Before the introduction of the lesion (B) the domain harbors three spirals with tip trajectories indicated in green and direction by arrows. After the lesion (C), a single activation front is stably anchored at the lesion, resulting in regular activation. Scalebars: 1 cm.

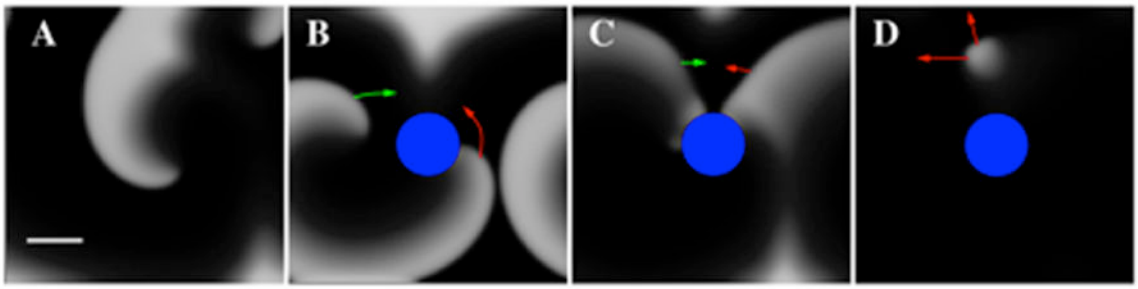

Figure 2.

An excitable gap created by ablation is invaded by fibrillatory waves to rapidly terminate spiral wave reentry. A. Multiple spiral waves exist prior to ablation. B. The abrupt creation of an ablation lesion (blue disk, non-conducting zone, R_{abl}=0.6 cm) leads to an activation front that rotates around the zone in a counter-clockwise fashion (indicated by red arrows) and an incoming wave (indicated by green arrows). C. The distance between the front and back of the wave is large enough that an incoming wave can excite the tissue. This results in a wave collision and dislodgement of reentry (D). Domain size 5cmx5cm, periodic boundary conditions in the horizontal direction. Scalebar: 1cm.

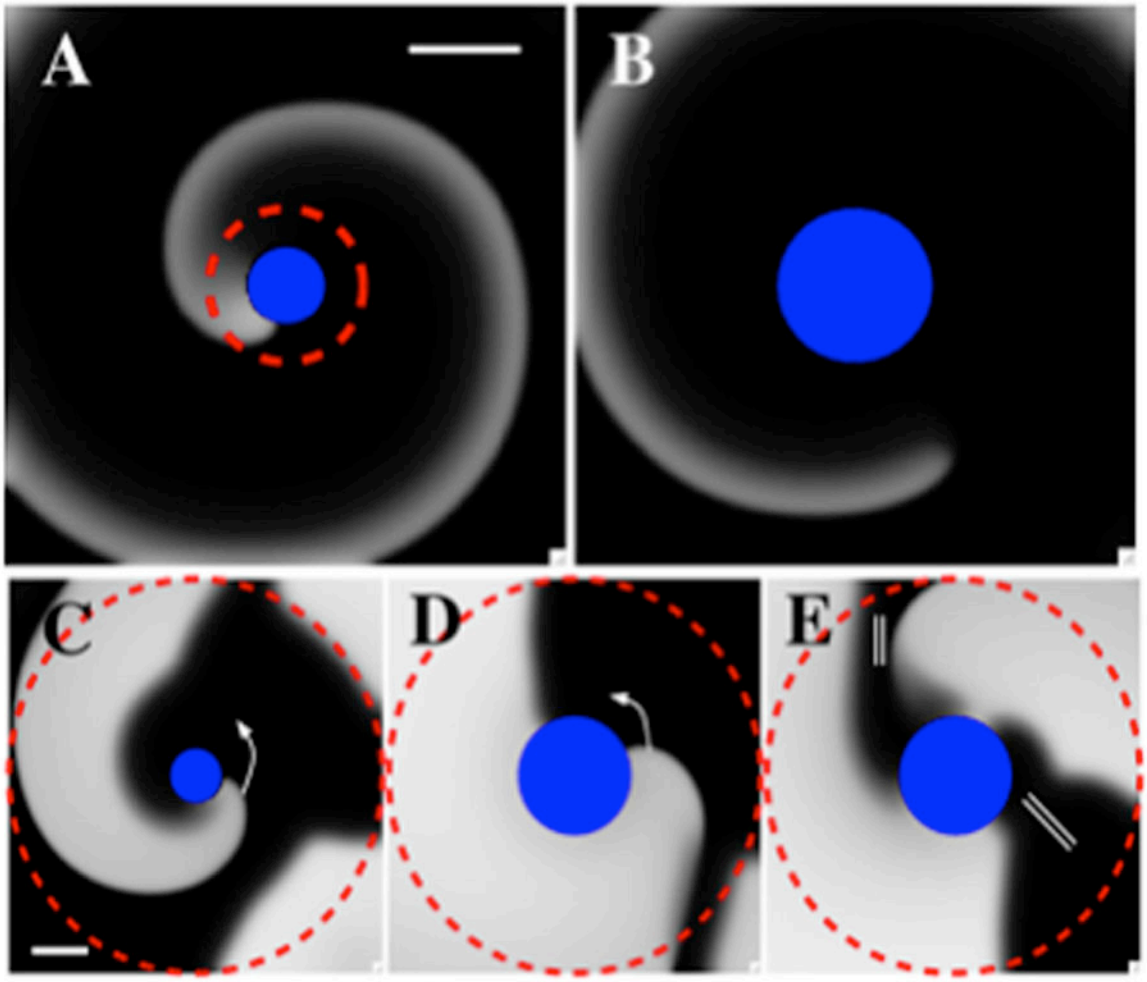

Figure 3.

Ablation of a spiral wave in tissue with heterogeneous excitability can result in wave detachment with subsequent termination. A–B: A region of high excitability (within dashed circle) surrounded by tissue with low excitability (tissue excitability falls linearly in the radial direction with R_1=0.4 cm, R_2=0.8 cm, τ_{d1} = 0.3 to τ_{d2} = 0.42, 5cmx5cm domain). A: Snapshot of an activation front attached to a non-conducting disk of radius R=0.4 cm while B: Snapshot of activation following ablation of the region of higher excitability (R_{abl}=0.8 cm). The wave front finds itself in a region of low excitability, detaches from the obstacle and migrates out of the computational domain, resulting in the termination of reentry. **C–E:** Ablation of a spiral wave in a region of low excitability. Tissue excitability within the dashed region varies radially and is lower closer to the obstacle (R_1=0.4 cm, R_2=2.5 cm, τ_{d1} = 0.35 to τ_{d2} = 0.25, 5cmx5cm domain). C: Snapshot of a counter clockwise rotating activation front attached to a non-conducting zone of radius R=0.4 cm. D, E: Snapshots of the activation following ablation of a disk (radius R_{abl}=0.8 cm). The wave front encounters the wave back, resulting in block, indicated by the double bar. The wave front subsequently detaches from the obstacle and migrates out of the computational domain, resulting in the termination of reentry (not shown). Scalebars: 1cm.

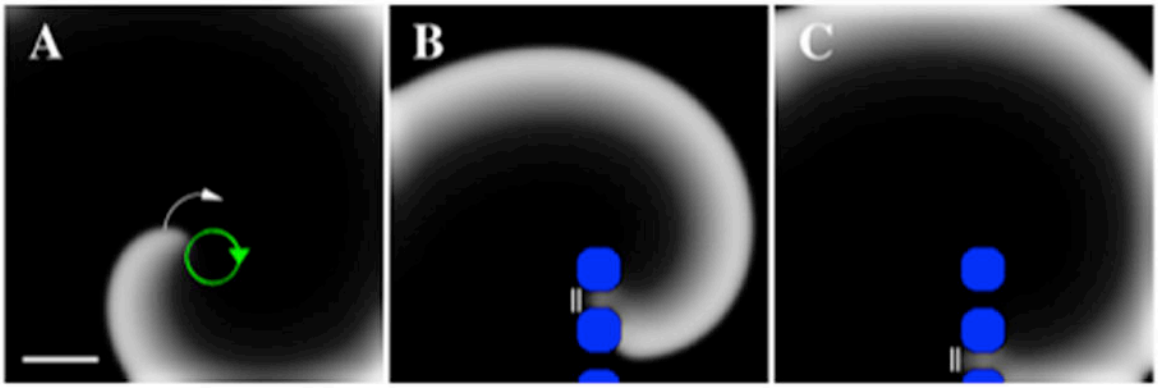

Figure 4.

Termination of spiral wave reentry by ablation connecting to a non-conducting boundary. A. Snapshot of a spiral wave before ablation, with the tip trajectory in green. Upon creating lesions (blue) placed on a line connecting the spiral tip domain to a non-conducting boundary, the spiral wave is blocked (B and C, indicated by the double bar), collides with the boundary and terminates (C). R_{abl}=0.4 cm, and domain size 5cmx5cm with no-flux boundary conditions. Note lesions do not have to overlap in order to block the wave and terminate reentry. Scalebar: 1cm.

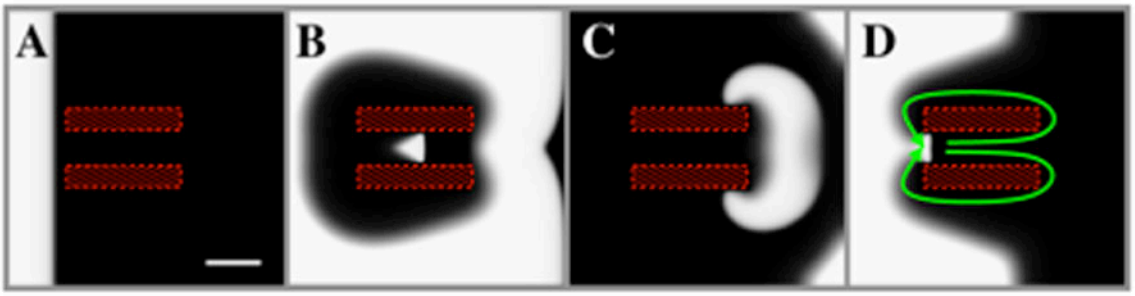

Figure 5.

Ablation of a slow-conducting isthmus can terminate spiral wave pairs. A. The hatched zones are non-conduction regions that sandwich an area of slow conduction, modeled as reduced cell-to-cell coupling that could biologically represent remodeled atrial tissue or patchy fibrosis. The mismatch in CV in this channel and the surrounding tissue creates a figure-of-eight reentry pattern, indicated by the green arrows in D. Domain size 5cmx5cm, D varies linearly in the isthmus from D=0.0002 cm2/ms (left-side) to D=0.00005 cm2/ms (right-side). Scalebar: 1cm.

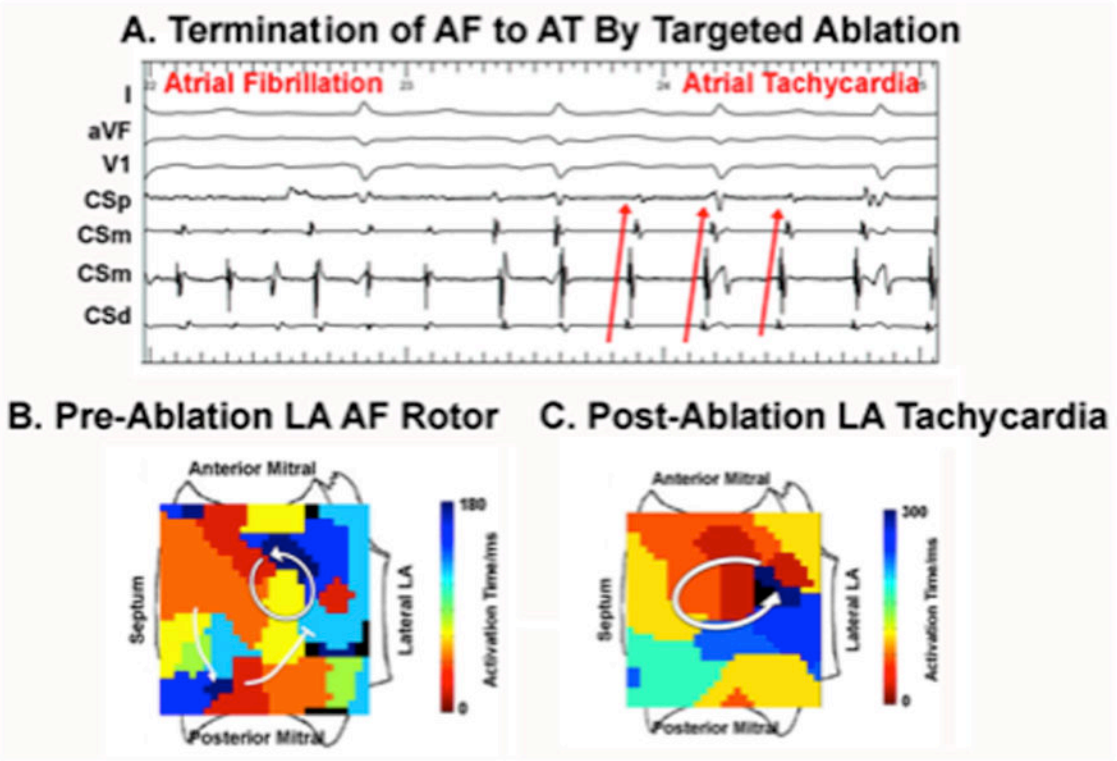

Figure 6.

Conversion of human AF to AT by localized ablation in left atrium. A. Electrograms show abrupt conversion. B. Pre-termination FIRM map shows counter clockwise AF rotor, as indicated by the arrow, with peripheral disorganization (fibrillatory conduction) in this chamber; C. Post-termination FIRM map shows AT at this location. Note cycle length prolongation and regular activation sequence in post ablation AT.

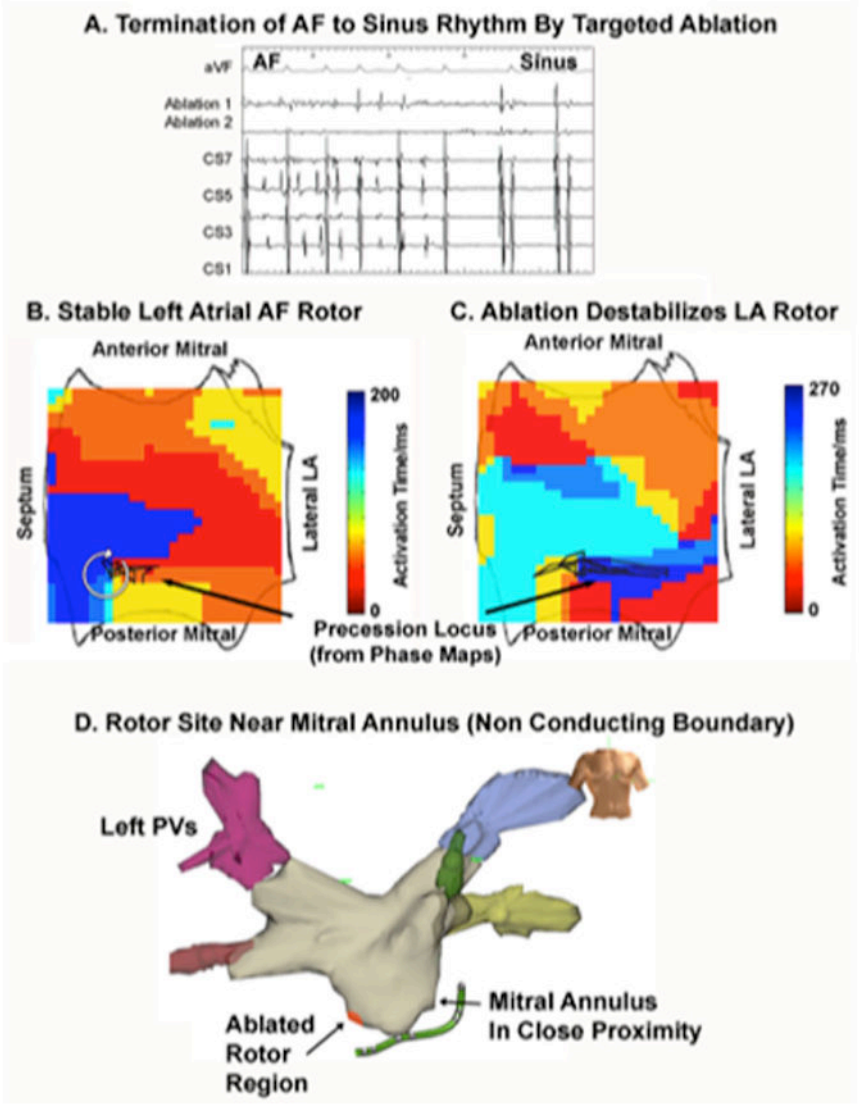

Figure 7.

Termination of AF to sinus rhythm by ablation that detaches AF rotor enabling its collision with nearby anatomic structures (mitral annulus or left inferior pulmonary vein orifice). (A) Intracardiac. (B) Clockwise rotor that precesses in a limited region of low left atrium before ablation; (C) Ablation de-stabilizes the rotor precession locus, causing AF to terminate to sinus rhythm. (D) Proximity of rotor to the mitral annulus, in particular, may have enabled rapid AF termination.

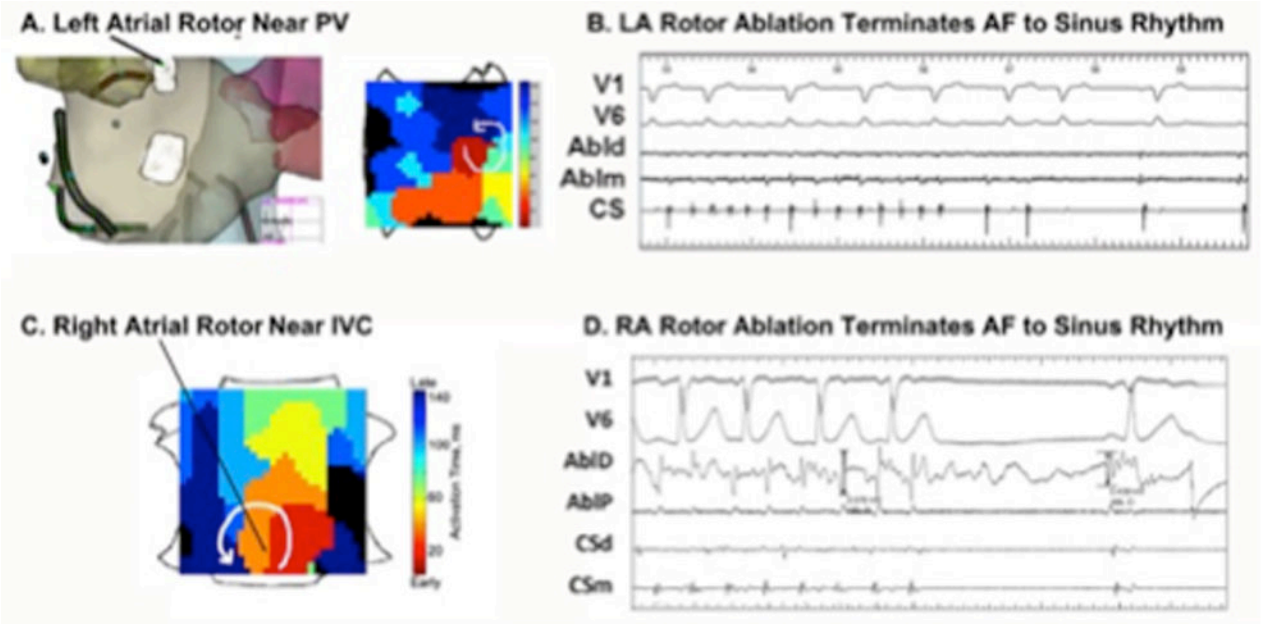

Figure 8.

Termination of human AF directly to sinus rhythm by targeting rotors near non-conducting boundaries, consistent with ablation connecting to the boundary. Elimination of a rotor near (A) Left inferior pulmonary vein (PV) in left atrium (subsequent ablation site also shown); (B) terminated AF to sinus rhythm; Ablation of rotor near (C) Inferior Vena Cava (IVC) in right atrium, (D) terminated AF abruptly to sinus rhythm.

Table 1

Numerical details

Mechanism	Figure	Domain size (cm)	Boundary conditions	τ_d
AF to AT	1	5x5 (A) 10x5 (B, C)	Non-conducting in all directions (A) Non-conducting in vertical and periodic in horizontal direction (B, C)	0.35
Excitable gap	2	5x5	Non-conducting in vertical and periodic in horizontal direction	0.34
Heterogeneous excitability	3	5x5	Non-conducting in all directions	0.30–0.42 (A, B) 0.35-0.25 (C–E)
Connection to non-conducting boundary	4	5x5	Non-conducting in all directions	0.38
Isthmus ablation	5	5x5	Non-conducting in all directions	0.30